

Dmitry S. Saiko¹ , Sergey A. Titov² , Igor A. Saranov² ,
Danila G. Andreev² , Natalja N. Lobacheva² 

¹Federal State Budget Educational Institution of Higher Education
"Voronezh State Technical University", Voronezh, Russian Federation;

²Federal State Budget Educational Institution of Higher Education
«Voronezh State University of Engineering Technologies», Voronezh, Russian Federation

(*Corresponding author's e-mail: mr.saranov@mail.ru)

Moisture Transfer During its Evaporation from Sugar Solutions

In this work, studies were carried out on the water evaporation from concentrated solutions of such sugars as sucrose, fructose, glucose, galactose, to determine the evaporation mechanisms. Differential scanning calorimetry (DSC) method in the temperature range from -70°C to $+200^{\circ}\text{C}$, as well as the combined thermogravimetric analysis with differential scanning calorimetry under isothermal conditions at temperatures of 30° , 45° , 60°C were used. The analysis of the DSC curves of sucrose solutions at low temperatures shows that in sugar solutions with a concentration of 65 %, water does not produce melting peaks. Therefore, it can be considered bound in the first hydration shells of sucrose. Isothermal thermogravimetric measurements give close to linear dependences of mass loss on time, and their slope being determined by temperature. At higher concentrations of sucrose solutions DSC curves for disaccharides are shifted relative to the curves for monosaccharides. This may be due to the lower permeability of the film surface for water. The evaporation model based on the vacancy mechanism of water molecules movement in concentrated sugar solutions was proposed. According to this model, the region enriched with vacancies of water molecules gradually penetrates deep into the sample. In this case, the number of water molecules in each layer of the region sets at a certain level. The given model constructions are applicable to the initial stages of water evaporation from concentrated sugar solutions.

Keywords: moisture, bond, sugar solutions, mathematical model, process, evaporation, thermal analysis, differential scanning calorimetry, differential thermal analysis, concentration, glass transition.

Introduction

The study of phase transitions, such as evaporation, and in particular water evaporation from various materials is one of the important problems of physical chemistry. It can be considered as moisture transfer from the liquid to the gas phase. This process is both of great theoretical and practical value.

The processes of moisture transfer and, in particular, evaporation, play an important role, for example, in food production. However, unlike many other cases of moisture transfer, for example, water evaporation from natural reservoirs, in food technology moisture is often transferred in systems containing not only free, but also the so-called bound water, that is, water present in the hydration shells of food material molecules. For example, the productivity of membrane technological processes, accompanied by the formation of polarization layers at the membrane boundary, depends directly on their rheological characteristics (viscosity, ultimate shear stress), which, in turn, depend on these particles hydration. Drying of food systems is greatly slowed down at a certain stage of dehydration, which is caused by some peculiarities of moisture transfer in materials containing bound water.

In recent years, bound water was actively studied by modern physical methods, such as X-ray microtomography, analysis of the microbalance of quartz crystals with a deposited material that binds water [1], absorption spectroscopy of electromagnetic radiation in the terahertz range [2], proton nuclear magnetic resonance [3], T -2 magnetic resonance relaxometry [4], etc.

Differential scanning calorimetry DSC [5] and differential thermal analysis DTA in combination with thermogravimetry are of special importance among the physical methods that can be effectively used for bound water characteristics measuring [6].

Isothermal DSC methods are of particular interest for the analysis of the bound water state [7]. They make it possible to choose the temperature which does not cause any structural transformations of the sample.

DSC is a very informative method for studying physical characteristics of intermolecular bonds in various materials. Thermal effects associated with phase transitions and chemical reactions depending on temperature are studied within the framework of this method. Information about the composition and thermophysical properties of food systems can be obtained with the help of DSC curve (heat flux versus temperature). Some researchers used DSC and DTA methods to study water binding in various food materials and additives, for example, in beef [8] and starch-gelatin food films [9]. Oxygen-functionalized porous activated bio-carbons with a large surface area obtained from grape seeds with the DSC method were studied in [10].

These bio-carbons are aimed to absorb CO₂ from the atmosphere. Samples with the largest surface area, pore volume, and the maximum number of surface oxygen functional groups showed the largest endothermic peak in terms of area according to DSC data, as well as the largest weight loss in the range of 80–100 °C.

The authors of [11] studied the sludge remaining after wastewater filtration by DTA and DSC methods. It was found out that the average binding power of water with the dry matter of sludge at a sufficiently high moisture content (above 50 %) ranges from 38 to 68 kJ/kg, depending on the type of sludge, and increases almost 10 times in the moisture range of 0–50 %.

Some modern thermal analysis instruments allow simultaneous thermal analysis (STA), i.e. combine the DSC or DTA method with the thermogravimetry (TG) method. Attempts to quantify bound water in food systems by this method were made earlier. Thus, in [12], thermogravimetry (TG) data were processed by the method of nonisothermal kinetics. It consisted of determining the logarithm dependence of the transformation degree α on temperature with thermogravimetric curves. The slope tangent of this graph, up to a constant factor, is equal to the amount of energy spent on the sample dehydration. The type of water binding with the material studied is determined by the range of dehydration powers. Therefore, this method can be used to characterize the distribution of water in a sample according to binding forms. However, an enormous spread in the values of kinetic parameters is considered to be one of the disadvantages of the non-isothermal approach [13].

However, there are no works using DSC and DTA methods that would clearly describe the mechanism of moisture transfer in systems with bound water.

The purpose of this work is to study a particular case of moisture transfer (evaporation) in systems with bound water, namely in concentrated solutions of food sugars such as sucrose, glucose, fructose, lactose, galactose.

Experimental

Samples of sugar solutions were produced in the laboratory at FSBEI HE VSUET (Federal State Budget Educational Institution of Higher Education “Voronezh State University of Engineering Technologies”).

DSC analysis at low temperatures and simultaneous thermal analysis (hereinafter STA) (DSC+TG) were performed on a STA 449 F3 Jupiter® simultaneous thermal analysis apparatus from NETZSCH (Germany). Calibration of the E-sensor by temperature and enthalpy taken from calibration substances (C10H16, C12H10, In, Bi, Zn) was previously carried out. Samples of raw materials weighing 15–22 mg were taken for analysis and placed in aluminum crucibles.

Differential scanning calorimetry (DSC) in the temperature range from –70° to +20° C, heating rate of 5 deg/min was used in the DSC method of analysis. The system was cooled with liquid nitrogen at a rate of 5 deg/min. The measurements were taken in a helium atmosphere (purge gas flow rate 10 ml/min, shield gas flow rate 10 ml/min). Temperature measurement accuracy was $\pm 0.3^\circ$ C.

Isothermal conditions at temperatures of 30°, 45°, 60° C were used in TG measurements. Measurements were carried out in the high-purity nitrogen atmosphere (purge gas flow rate 50 ml/min, shielding gas flow rate 10 ml/min).

Isothermal conditions at temperatures of 30°, 45°, 60° C were used for STA (TG+DSC) measurements. The measurements were taken in high-purity nitrogen atmosphere (purge gas flow rate 50 ml/min, shielding gas flow rate 10 ml/min).

Statistical processing of the experimental results was carried out as follows.

The experiment standard error was determined by the formula:

$$S.E. = \sqrt{\frac{\sum_{s=1}^m \sum_{i=1}^n y_{is}^2}{(n_y - 1)(n_y)}}$$

where s is the number of array; i is the number of point in the array; m is the array number for point y on the chart; n is the number of points in each array; y_{is} is the data value of array s and i -th point; n_y is the total number of data values in all arrays.

Results and Discussion

Studies by differential scanning calorimetry method at low temperature were carried out to determine the concentration of sugar solutions at which all water molecules are bound in the first hydrate shells.

The results of differential scanning calorimetry of a 45 % sucrose solution are shown in Figure 1.

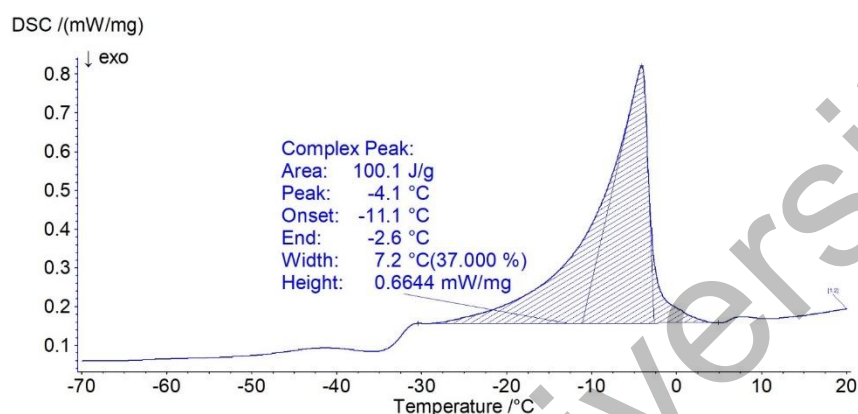


Figure 1. Thermogram of a 45 % mass concentration of sucrose solution melting DSC, mW/mg·10²

As can be seen in Figure 1, the frozen sucrose solution melts in the temperature range of $-35...0$ °C, and the largest area of the melting peak falls in the range of $-7...-3$ °C. Comparing the peak melting area for the sigmoidal baseline (100.1 J/g of solution) with the corresponding pure water surface area (334.3 J/g), we come to conclusion that it is only 0.30 of this value.

Taking into account the water content in a 45 % sugar solution and comparing the peak areas, we obtain approximately 55 % of the water frozen and then melted in this solution. The rest part is non-frozen and considered to be bound water.

The DSC curve for a 65 % sugar solution (Fig. 2) shows the presence of two exo- and endothermic peaks of approximately the same area. These areas are very small compared to the peaks corresponding to ice melting. This dependence is characteristic of the glass transition of a sugar solution [14] and is not directly related to water melting. Therefore, we can conclude that all water is in a bound state in a 65 % solution.

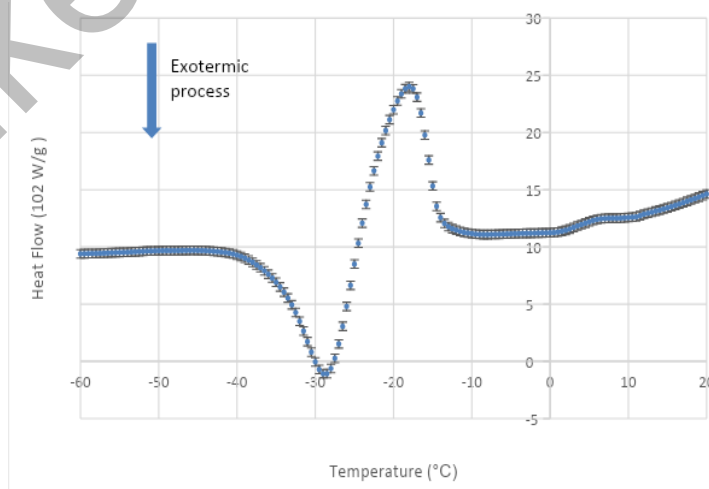


Figure 2. Thermogram of a 65 % mass concentration of sucrose solution melting

If we count the number of water molecules bound with hydroxyl groups per one sucrose molecule, their mass assessment will give about 35 % of the entire solution mass, i.e. all water in the 65 % sugar solution is hydrogen bonded to sucrose.

TG measurements in isothermal mode were also carried out. To do this, a container with a sugar solution was placed in the measuring cell of the calorimeter, which was openly placed in a nitrogen atmosphere and thermostated at a temperature of $T_1 = 29\text{ }^\circ\text{C}$. The sample mass relative to the initial mass was recorded as a function of time (the value of TG in Fig. 3).

Figure 3 shows that the sample temperature sets at a level close to $29\text{ }^\circ\text{C}$ in approximately 12 minutes after the experiment start.

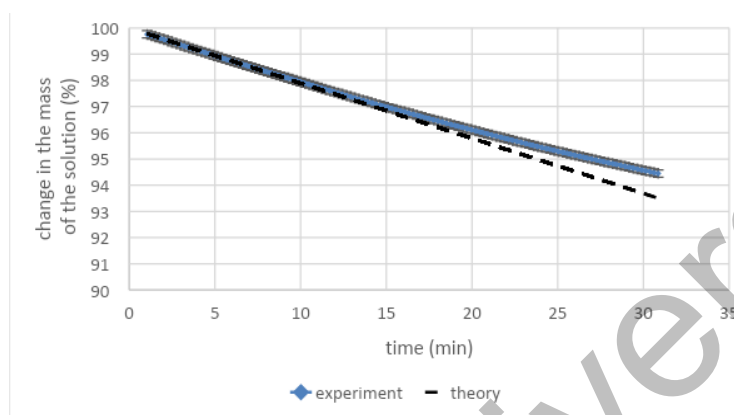


Figure 3. TG measurements in the isothermal mode of a sucrose solution with a mass concentration of 65 % at $30\text{ }^\circ\text{C}$

In practice, water evaporation usually occurs from systems containing both bound and free water. Therefore, we took isotherms of water evaporation from solutions of various sugars with a concentration of 20 % at a raised temperature. Under such conditions, water from the crucible is almost completely evaporated during the experiment, i.e., the solution concentration increases with time due to evaporation.

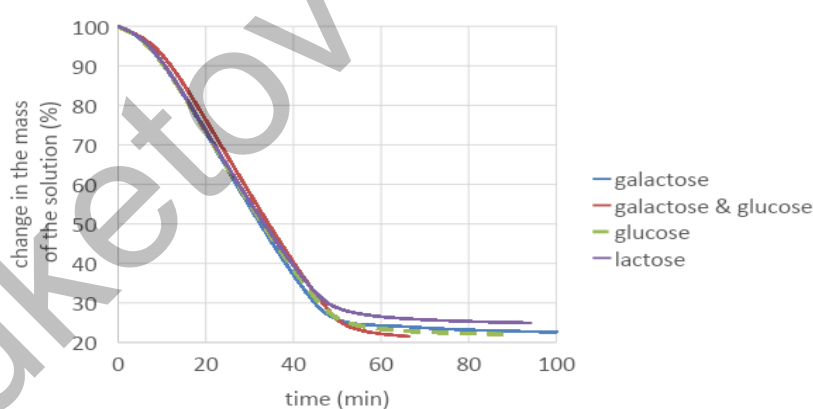


Figure 4. Results of simultaneous thermal analysis (TG + DSC) of measurements of sugar solutions with a mass concentration of 18 % at a temperature of $60\text{ }^\circ\text{C}$

Figure 4 shows that the curves slope remains constant both over time and for different sugars up to a sugar concentration of 60–70 %. However, the slope of m versus t graph turns out to be smaller than that one for distilled water under the same conditions (Fig. 5). The reason for this phenomenon requires further research. However, a monolayer sugar film is possible to be formed on the surface of solutions with a weak concentration, preventing partially the evaporation of water. The level at which the mass stabilizes at an evaporation time of more than 50 minutes is different for all solutions. It is the highest for lactose solution. This means that a certain amount of water still remains in it after the end of active evaporation.

Great differences between sugars appear at 62–67 % solutions concentration. This is especially evident in the DSC curves. The amount of heat used to evaporate moisture decreases rapidly at a certain concentra-

tion due to a sharp drop in the evaporation rate. The DSC curve for lactose disaccharide runs more to the left than for a mixture of lactose and galactose monosaccharides. A similar pattern is observed for sucrose and its hydrolysis products — glucose and fructose (Fig. 5).

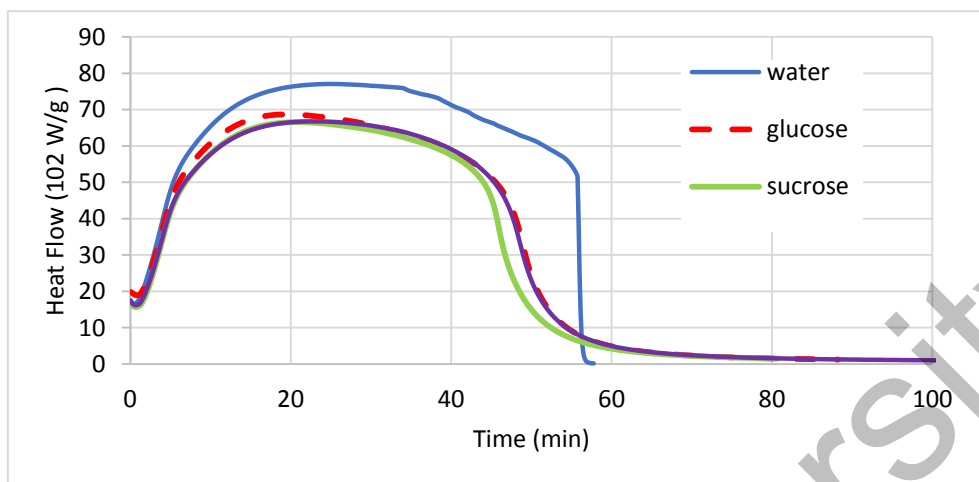


Figure 5. DSC curves of 20 % mass concentration of sugar solutions and distilled water at 60 °C

This means that unlike monosaccharides a dense, weakly permeable film begins to form on disaccharide solutions surface at a lower concentration. In other words, disaccharides films are less permeable to water at the same concentration.

Let us present some model ideas about the evaporation process from such solutions.

Let there be a solution where all water molecules are bound in sugar molecules first hydrate shells, i.e., they are attached to the hydroxyl groups of the sugar molecule by a hydrogen bond. Since water molecules are much smaller than sugar molecules, let us imagine the sugar molecules as immobile, and the water molecules moving relative to them and then moving into the gas phase in the process of evaporation. Water molecules movement can be as follows in such a system. If a water molecule leaves the solution due to evaporation, a vacancy forms in the hydrate shell of the sugar molecule. It is filled with a water molecule from the hydrate shell of the same or neighboring sugar molecule, leaving a vacancy filled by the next water molecule, and so on. That is, the sucrose molecules hydroxyl groups, to which water molecules can be attached by hydrogen bonds, can be represented as a positions grid that can or cannot be filled with water molecules.

Let us consider the solution volume, imagining the evaporation mechanism as shown in Figure 6. There are fixed positions, marked with light circles, in which molecules can reside (dark circles).

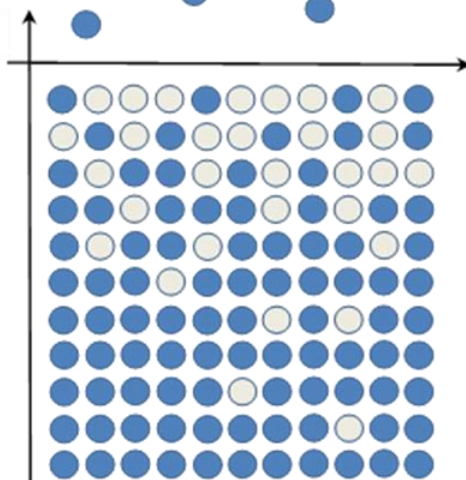


Figure 6. Graphical representation of the mechanism of evaporation from sugar solutions

As an initial approximation, we accept that a molecule transition in some characteristic time is possible only horizontally and vertically to an unoccupied place. Let N_0 be the total number of seats in one layer, N_i be the number of occupied seats in the layer with number i . Let there be three probabilistic parameters:

- probability r of the molecule exit from the first layer into the gas;
- probability p of a molecule transition from one layer to another, and the motion direction along the z axis does not matter;
- probability s of a molecule transition within one layer.

Let us consider changes kinetics in the population of layer i in one “cycle” of time. We will take the directions as shown in Figure 7.

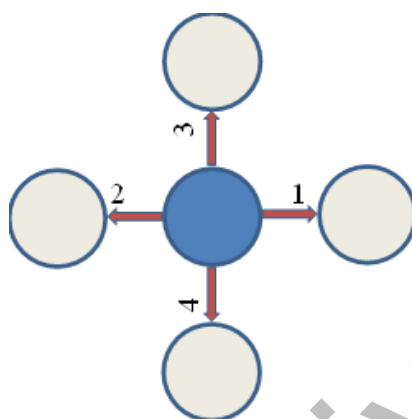


Figure 7. Graphical representation of the directions of the layer i population for one time “cycle”

The probabilities that the positions indicated in the figure will be free are, respectively, for positions 1 and 3: $1 - \frac{N_i - 1}{N_0} \approx 1 - \frac{N_i}{N_0}$; for position 2: $1 - \frac{N_{i-1}}{N_0}$; for position 4: $1 - \frac{N_{i+1}}{N_0}$.

Let us take into account the probabilities of molecular migrating accepted in the model. Then, with a one-step movement, we get:

$$\Delta N_i = N_0 p \cdot \left(\frac{N_{i-1}}{N_0} \left(1 - \frac{N_i}{N_0} \right) + \frac{N_{i+1}}{N_0} \left(1 - \frac{N_i}{N_0} \right) - \frac{N_i}{N_0} \left(1 - \frac{N_{i-1}}{N_0} \right) - \frac{N_i}{N_0} \left(1 - \frac{N_{i+1}}{N_0} \right) \right). \quad (1)$$

Let us take into account the probabilities of molecular migrating accepted in the model. Then, with a one-step movement, we get:

$$\Delta N_1 = N_0 p \cdot \left(\frac{N_2}{N_0} \left(1 - \frac{N_1}{N_0} \right) - \frac{N_1}{N_0} \left(1 - \frac{N_2}{N_0} \right) \right) - N_0 r \cdot \frac{N_1}{N_0}. \quad (2)$$

After simplification, we obtain the system of equations

$$\begin{aligned} \Delta N_i &= p (N_{i-1} + N_{i+1} - 2N_i); \\ \Delta N_1 &= p \cdot (N_2 - N_1) - rN_1. \end{aligned} \quad (3)$$

After introducing the notation $v_i = \frac{N_i}{N_0}$, these equations can be written as differential equations

$$\left\{ \frac{dv_i}{dt} = -p(2v_i - v_{i-1} - v_{i+1}); \frac{dv_1}{dt} = -p(v_1 - v_2) - rv_1; v_\infty(t) = 1. \right. \quad (4)$$

It is easy to write the system of equations for three layers together with the initial and boundary conditions in an explicit form:

$$\left\{ \frac{d}{dt} v_1(t) = -p(v_1(t) - v_2(t)) - rv_1(t), \frac{d}{dt} v_2(t) = -p(v_2(t) - v_1(t)) - v_3(t), v_1(0) = 1, v_2(0) = 1, v_3(0) = 1 \right\} \quad (5)$$

The third layer is assumed to be always filled. We can write the solution in the form:

$$v_1(t) = \frac{p+r \cdot e^{-\frac{1}{2}(3p+r)t} \left(2ch(tq) + \frac{2p-r}{q} sh(tq) \right)}{p+2r}; \quad (6)$$

$$v_2(t) = \frac{p+r \cdot e^{-\frac{1}{2}(3p+r)t} \left(ch(tq) + \frac{3p+r}{2q} sh(tq) \right)}{p+2r}, \quad (7)$$

where the q parameter is:

$$q = \frac{1}{2} \sqrt{5p^2 - 2pr + r^2}.$$

Graphs for arbitrarily chosen values of the parameters $p = 0.03$, $r = 0.1$ are shown in Figure 8.

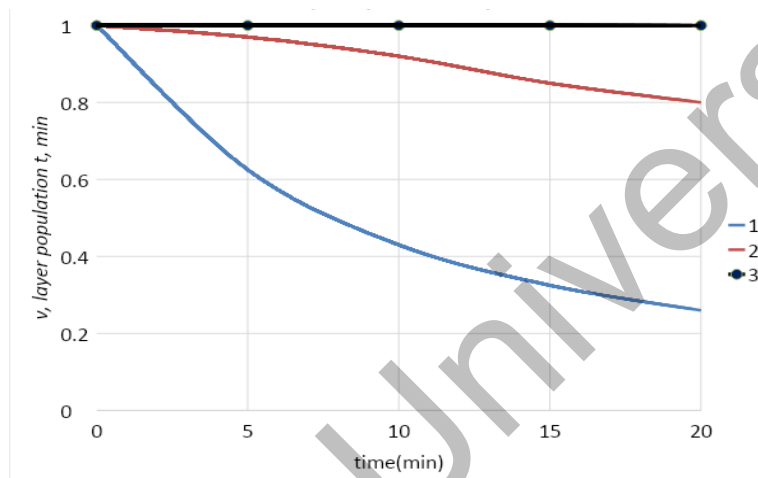


Figure 8. Graphs of the dependence of layers 1, 2 and 3 population on time (s)

Figure 8 shows that the number of molecules in the first layer tends to a certain stationary value in the interval of 0–20 minutes. That is, in some time after the process start, we can assume that $\frac{\partial v_1}{\partial t} = 0$.

At the same time, the number of water molecules in the second layer decreases in this time interval, while in the third layer it remains at the maximum level. This means that the front of the area depleted of water molecules penetrates gradually deep into the sample, the number of water molecules in each layer of this area setting at a certain level.

The probability r included in system (5) can be expressed in terms of the binding power of water with a sucrose molecule in a layer of sucrose solution adjoining air with the Boltzmann distribution:

$$r = e^{-\frac{U_1}{kT}}. \quad (8)$$

In this case, a water molecule bound to a sucrose molecule is represented as a particle in a potential well with depth U_1 , where U_2 is the binding power of a water molecule with a sucrose molecule

The probability p can be expressed in a similar way:

$$p = e^{-\frac{U_2}{kT}}. \quad (9)$$

Here U_2 is the binding power of a water molecule with a sucrose molecule in the solution second layer. Let us introduce the value θ as the ratio of the number of molecules leaving the layer to the total number of molecules in the layer:

$$\theta = \frac{\Delta N}{N_0}, \quad (10)$$

where ΔN is the number of molecules leaving the layer in some time τ_0 , equal to the particle oscillation period in the potential well.

Expressing θ in terms of water mass Δm leaving the layer in time τ_0 and the water molecule mass $m_{.M6}$, we obtain:

$$\theta = \frac{\Delta m}{m_{.M6} N_0}. \quad (11)$$

On the other hand, it is obvious that:

$$\theta = v_1 r. \quad (12)$$

Taking into account expressions (10)–(12), for the stationary case, the solution of the system of equations (5) is as follows:

$$\left(\frac{1}{\tau_0 \theta} - e^{\frac{u_1}{kT}} \right) e^{\frac{u_2}{kT}} = 2. \quad (13)$$

If the evaporation process is carried out at temperatures T_1 and T_2 , then the following equations will take place in the first and the second cases, respectively:

$$\frac{1}{\tau_{01} \theta_1} - e^{\frac{u_1}{kT_1}} = 2e^{\frac{-u_2}{kT_1}}; \quad (14)$$

$$\frac{1}{\tau_{02} \theta_2} - e^{\frac{u_1}{kT_2}} = 2e^{\frac{u_2}{kT_2}}.$$

Here θ_1 and θ_2 are the values determined by formula (11) by the mass loss of the sample at temperatures T_1 and T_2 , respectively. Having determined their values from the experiment and taking into account (11), we can find the binding powers u_1 and u_2 , and then the values r and p respectively with formulas (14).

The value Δm included in equation (11) can be determined from the slope of the experimental graph $m(t)$ during 12–15 minutes from the start of the experiment.

Substituting the obtained values Δm_1 for a temperature of 29 °C and Δm_2 for a temperature of 45 °C into formula (11), and solving the system of equations (14), we obtained the following values of the binding power of water with a sucrose molecule in the layer, adjacent to air $U_1 = 2875$ J/g and in the second layer $U_2 = 3520$ J/g.

In this case, the characteristic period of thermal vibrations of a water molecule near a sucrose molecule was $\tau_0 = 0,32 \cdot 10^{-8}$ c.

The theoretical graph $m(t)$, built with the found values, is shown in Figure 8.

It is linear, while the slope of the experimental graph decreases with time. This means that the above considerations can be applied to the initial stages of the evaporation process. Apparently, at a sufficiently large depletion area width, stationary diffusion of water molecules occurs through the depletion area. However, it is necessary to choose the vacancy mechanism for the movement of water molecules in solution as a basis for diffusion describing process. To build a theoretical graph of m versus t , for example, for sucrose solutions, it is necessary to know the specific values of p and r for solutions of a certain concentration.

The binding powers values obtained here are approximate, since it is not known exactly which part of the curve Δm versus t corresponds to the stationary filling of the upper layer. However, it is obvious that E_{cs} in the sample depth is much larger than that one on the surface.

One water molecule falls on one OH- group of the disaccharide molecule at concentrations of 62–67 %. This means that if at lower concentrations there is free water, which is not bound to hydroxyl groups, in the surface film, then in this case, on the contrary, vacancies of water molecules appear in hydrate shells of sugar molecules. At the same time the mechanism of water diffusion through the surface film changes greatly.

The water molecule evaporates, forming a vacancy in the hydrate shell of the sugar molecule. A molecule of water occupies the vacated seat from the hydrate shell of the neighboring sugar molecule. Then another water molecule gets there, and thus the diffusion flow of water from the depth to the surface of the solution goes. Since disaccharide molecules are larger than monosaccharide molecules, in the first case,

the water molecule moves mainly from one OH-group to another within one molecule. And only after a few jumps they move on to another. And in the second case, the number of jumps from one molecule to another is greater. It is possible that the stereometry of the molecules in the film is such that the latter transition is more probable. Then the diffusion coefficient of water in monosaccharides films will be higher than in the case of disaccharides, which is observed experimentally.

Conclusions

Thus, the results of the work show that the parameters of bound water transfer can be determined from dehydration isotherms not only at the boundary with the gas phase, but also in the bulk of the water-binding material. The vacancy mechanism of moisture movement in high concentration sugar solutions was proposed and mathematically substantiated in the work. The surface film with an increased concentration of sugar in the case of disaccharides solutions is less permeable to water than to monosaccharides.

Acknowledgments

The authors appreciate the Center for Collective Use “Test Center” on the basis of the FSBEI HE VSUET (Federal State Budget Educational Institution of Higher Education “Voronezh State University of Engineering Technologies”) for organizing and supporting research with its own material base and the assistance of Specialists.

References

- 1 Rudolph, G., Hermansson, A., Jönsson, A. S., & Lipnizki, F. (2021). In situ real-time investigations on adsorptive membrane fouling by thermomechanical pulping process water with quartz crystal microbalance with dissipation monitoring (QCM-D). *Separation and Purification Technology*, 254, 117578. <https://doi.org/10.1016/j.seppur.2020.117578>
- 2 Liang, W., Zuo, J., Zhou, Q., & Zhang, C. (2022). Quantitative determination of glycerol concentration in aqueous glycerol solutions by metamaterial-based terahertz spectroscopy. *Spectrochimica Acta Part A: Molecular and Biomolecular Spectroscopy*, 270, 120812. <https://doi.org/10.1016/j.saa.2021.120812>
- 3 Yoshida, T., Okabayashi, H., Takahashi, K., & Ueda, I. (1984). A proton nuclear magnetic resonance study on the release of bound water by inhalation anesthetic in water-in-oil emulsion. *Biochimica et Biophysica Acta (BBA)-Biomembranes*, 772(1), 102–107. [https://doi.org/10.1016/0005-2736\(84\)90522-4](https://doi.org/10.1016/0005-2736(84)90522-4)
- 4 Khan, M. I. H., Wellard, R. M., Nagy, S. A., Joardder, M. U. H., & Karim, M. A. (2016). Investigation of bound and free water in plant-based food material using NMR T2 relaxometry. *Innovative food Science & emerging technologies*, 38, 252–261. <https://doi.org/10.1016/j.ifset.2016.10.015>
- 5 Hempel, N. J., Brede, K., Olesen, N. E., Genina, N., Knopp, M. M., & Löbmann, K. (2018). A fast and reliable DSC-based method to determine the monomolecular loading capacity of drugs with good glass-forming ability in mesoporous silica. *International journal of pharmaceutics*, 544(1), 153–157. <https://doi.org/10.1016/j.ijpharm.2018.04.035>
- 6 Mukasyan, A. S. (2017). DTA/TGA-based methods. In *Concise Encyclopedia of Self-Propagating High-Temperature Synthesis* (pp. 93–95). Elsevier. <https://doi.org/10.1016/B978-0-12-804173-4.00040-5>
- 7 Joyce, K., Rahmani, S., & Rochev, Y. (2020). Quasi-isothermal modulated DSC as a valuable characterization method for soft tissue biomaterial crosslinking reactions. *Bioactive Materials*, 5(2), 428–434. <https://doi.org/10.1016/j.bioactmat.2020.03.002>
- 8 Ma, C. Y., & Harwalkar, V. R. (1991). Thermal analysis of food proteins. In *Advances in food and nutrition research* (Vol. 35, pp. 317–366). Academic Press. [https://doi.org/10.1016/S1043-4526\(08\)60067-4](https://doi.org/10.1016/S1043-4526(08)60067-4)
- 9 Al-Hassan, A. A., & Norziah, M. H. (2012). Starch–gelatin edible films: Water vapor permeability and mechanical properties as affected by plasticizers. *Food hydrocolloids*, 26(1), 108–117. <https://doi.org/10.1016/j.foodhyd.2011.04.015>
- 10 Ismail, I. S., Singh, G., Smith, P., Kim, S., Yang, J. H., Joseph, S., & Vinu, A. (2020). Oxygen functionalized porous activated biocarbons with high surface area derived from grape marc for enhanced capture of CO₂ at elevated-pressure. *Carbon*, 160, 113–124. <https://doi.org/10.1016/j.carbon.2020.01.008>
- 11 Deng, W., Li, X., Yan, J., Wang, F., Chi, Y., & Cen, K. (2011). Moisture distribution in sludges based on different testing methods. *Journal of Environmental Sciences*, 23(5), 875–880. [https://doi.org/10.1016/S1001-0742\(10\)60518-9](https://doi.org/10.1016/S1001-0742(10)60518-9)
- 12 Zvetkov, V. L., Simeonova-Ivanova, E., & Calado, V. (2014). Comparative DSC kinetics of the reaction of DGEBA with aromatic diamines IV. Iso-conversional kinetic analysis. *Thermochimica Acta*, 596, 42–48. <https://doi.org/10.1016/j.tca.2014.09.014>
- 13 Kramarenko, V. Yu. (2013). Nonisothermal kinetics in the thermal analysis of polymers. 1. Simple reactions. *Bulletin of the National Technical University KhPI. Series: Chemistry, chemical technology and ecology*, (64), 64–76.
- 14 Mahato, S., Zhu, Z., & Sun, D. W. (2019). Glass transitions as affected by food compositions and by conventional and novel freezing technologies: A review. *Trends in Food Science & Technology*, 94, 1–11. <https://doi.org/10.1016/j.tifs.2019.09.010>

Information about authors*

Saiko, Dmitry Sergeevich — Doctor of Physical and Mathematical Sciences, Professor, Professor of the Department of Higher Mathematics and Physical and Mathematical Modeling, Voronezh State Technical University, Moskovsky av, 14, 394006, Voronezh, Russian Federation; e-mail: imanovaa@mail.com; <https://orcid.org/0000-0001-7116-4633>;

Titov, Sergey Aleksandrovich — Doctor of Technical Sciences, Professor, Department of Physics of Heat Engineering and Heat Power Engineering, Federal State Budget Educational Institution of Higher Education “Voronezh State University of Engineering Technologies”, Revolution av., 394036, Voronezh, Russian Federation; e-mail: 125titov@mail.ru; <https://orcid.org/0000-0003-1612-0018>;

Saranov, Igor Aleksandrovich (*corresponding author*) — Candidate of Technical Sciences, Senior Lecturer, Department of Information Security, Federal State Budget Educational Institution of Higher Education “Voronezh State University of Engineering Technologies”, Revolution av., 394036, Voronezh, Russian Federation; e-mail: mr.saranov@mail.ru; <https://orcid.org/0000-0002-9510-5168>;

Andreev, Danila Gennadievich — Graduate student, Department of Physics of Heat Engineering and Heat Power Engineering, Federal State Budget Educational Institution of Higher Education “Voronezh State University of Engineering Technologies”, Revolution av., 394036, Voronezh, Russian Federation; e-mail: peas_scalemodel@mail.ru; <https://orcid.org/0000-0003-4720-8362>;

Lobacheva, Natalja Nikolaevna — Candidate of Technical Sciences, Docent, Department of Foreign Languages, Federal State Budget Educational Institution of Higher Education “Voronezh State University of Engineering Technologies”, 19, Revolution av., Voronezh, 394036, Russian Federation; e-mail: naloni@mail.ru; <https://orcid.org/0000-0002-6561-7285>

*The author's name is presented in the order: *Last Name, First and Middle Names*